Chem. Senses 28: 807–815, 2003 DOI: 10.1093/chemse/bjg074

Coupling between Sensory Neurons in the Olfactory Epithelium

Rona J. Delay[1] and Vincent E. Dionne[2]

[1]Department of Biology, University of Vermont, Burlington, VT 05405, USA and [2]Department of Biology, Boston University, Boston, MA 02215, USA

Correspondence to be sent to: Dr Vincent E. Dionne, Department of Biology, Boston University, 5 Cummington Street, Boston, MA 02215, USA. e-mail: vdionne@bu.edu

Abstract

Coupling of olfactory sensory neurons (OSNs) in the olfactory epithelium of *Necturus maculosus* was demonstrated by dye-transfer with Lucifer yellow CH; however, the incidence of dye-transfer was low. Immunocytochemistry and Western blot analysis indicated that connexin 43, a gap junction channel subunit, was widely expressed by cells in the olfactory epithelium. Electrical coupling by presumptive gap junctions was assessed using electrophysiological recordings, heptanol block, tracer-uptake through hemi-junctions, and tracer-injection into tissue whole-mounts. Coupling, which involved pairs of OSNs only, was detected in ~3–10% of the OSN population; there was no evidence that OSNs were coupled into extended neural syncitia. These results suggest that coupling of OSNs by gap junctions is unlikely to have a general role in olfactory responses by mature (odor responsive) OSNs. Instead, the incidence of inter-neuronal coupling was small, similar to the fraction of immature OSNs, suggesting a possible role of gap junctions in the continual turnover and development of OSNs or possibly their senescence.

Key words: coupling, dye transfer, gap junction, olfactory epithelium, OSNs

Introduction

Gap junctions provide a pathway for intercellular communication, offering cytoplasmic continuity and electrical coupling between cells in many tissues including the olfactory epithelium of the nasal mucosa (Bruzzone *et al.*, 1996; Goodenough *et al.*, 1996). In the olfactory epithelium, gap junction channels can be found both in sensory neurons and non-neuronal cells (Miragall *et al.*, 1992; Menco, 1988). When expressed in olfactory sensory neurons (OSNs), the channels couple OSNs to one another as well as to sustentacular and basal cells (Schwartz Levey *et al.*, 1992). Recent immunohistochemical studies suggest that the protein subunits of gap junction channels are widely expressed by OSNs (Zhang *et al.*, 2000; Zhang and Restrepo, 2002, 2003); yet, the extent of functional coupling and the role of gap junction channels in OSNs remain unknown. In other neurons gap junctions have been principally associated with the control of local circuit architecture, as in the retina (Baldridge *et al.*, 1998), and with neuronal development (Sutor, 2002); both roles are possible in OSNs.

Mature OSNs detect, discriminate and communicate odor information, yet not all OSNs in the adult olfactory epithelium are mature. Unlike most neurons, OSNs survive only a few months, necessitating the continual birth and development of new neurons (Graziadei and Monti Graziadei, 1976; Weiler and Farbman, 1997). The development of a mature OSN requires about one week during which the cell acquires a chemosensory phenotype, extends an axon to the olfactory bulb, and establishes appropriate synaptic connections. In adult olfactory tissues ~90–95% of the OSNs are functionally mature at any time, suggesting that if gap junction channels have a role in the function of mature OSNs, the channels should be present in most of the cells.

We have examined the incidence of gap junction channels in the olfactory epithelium of the salamander *Necturus maculosus*. Using immunocytochemistry and Western blot analysis, connexin 43 (Cx43), a gap junction channel subunit, appears to be widely expressed in *Necturus* olfactory epithelium; however, functional coupling of OSNs appears to be limited to a small percentage of cells, consistent with a role in neuronal differentiation and development but inconsistent with a general role in the odor response or any other function common to mature OSNs.

Methods

In vitro epithelial preparation

Adult animals (*Necturus maculosus*) were anesthetized by immersion in ice water then decapitated. All procedures were approved by the institutional animal use committee. The olfactory mucosa was removed by blunt dissection, the mucosal tube split open along the medial edge, and pieces of the superficial layer of the epithelium carefully isolated.

Tissues from animals of either sex were used with no apparent differences.

Cell dissociation

Dissociated cells were isolated without degradative enzymes by briefly exposing small pieces of olfactory epithelium to low-calcium saline at basic pH and tuiturating them (Dubin and Dionne, 1993). The cell suspension was returned to normal physiological saline containing DNase, then held on ice until use.

Loading

Aliquots of 50–100 ml of dissociated cells in APS were plated on Cell-Tak-coated hematocrit chambers, and allowed to settle and adhere for 20 min. The cells were then incubated in low calcium (<100 nM) APS at pH 7.2 with 1% Lucifer yellow CH for 10 min then washed 3× with normal APS and counted; paired controls were incubated in normal APS with 1% Lucifer yellow CH and otherwise treated the same.

Slice preparation

The olfactory epithelium was removed by blunt dissection, cut open along one lateral edge, and glued to a substrate with its apical surface up. Slices 200–300 μm thick are cut using the method of Bigiani and colleagues (Bigiani and Roper, 1991, 1995). When kept at 4°C in saline, the cells remained viable for >24 h. Examination of the slices showed aggregates of OSNs, sustentacular cells and basal cells in pear-shaped clusters surrounded by ciliated respiratory epithelial cells.

Western blots

The nasal sacks were removed from the animal and homogenized. After solublization for 1 h the samples were spun at 3000 *g* at 4°C for 10 min. The supernatant was collected, 6× Laemelli buffer was added with 2-mercaptoethanol, and the resultant mixture was boiled for 5 min. The samples were run on a 10% SDS–polyacrylamide gel and transferred onto nitrocellulose membranes. The membranes were blocked overnight in a 5% dry milk/TBST (16 mM Tris–HCl, 4 mM Tris base, 137 mM NaCl, 1% Tween 20) solution at 4°C. After washing with TBST, the membranes were incubated in anti-Cx43 (Alpha Diagnostic, San Antonio, TX; CX43C13-M, lot XS8093) in TBST 1:1000 for 2 h at room temperature. After washing in TBST the blots were incubated with an anti mouse alkaline phosphatase conjugated secondary antibody (Sigma, A-3688, lot 61K9260) for 1 h at room temperature. The blots were visualized with alkaline phosphatase.

For the peptide competition, the Cx43 antibody was preincubated overnight at 4C in 20 μl of control peptide (Alpha Diagnostic, CX43C13-P); antibody for the positive control was preincubated in water without the peptide. These preabsorbed antibody preparations were then used as above. The positive control was developed until the band of interest was visualized, then the experimental was developed for an equal amount of time.

Immunocytochemistry

The nasal sacs were fixed in 2% paraformaldehyde in PBS (pH 7.2) overnight, washed and cytoprotected through a graded sucrose series (0.5, 1.0, 1.5, 2.0 M) and sectioned at 30 μm. The sections were blocked in preincubation buffer for 1–2 h (0.5% Triton X-100, 3% normal donkey serum in PBS). The primary antibody (anti-CX43 mouse antibody from Alpha Diagnostics) was diluted 1:1000 in pre-incubation buffer and the sections incubated for 2–3 days. The control sections were treated in the same manner but without primary antibody. After washing with PBS the sections were treated with the secondary antibody (Alexa Fluor 488 donkey anti-mouse, Molecular Probes A11034) for 1 h followed by PBS washes. Sections were viewed with fluorescent optics on a Zeiss Axioskop-2 microscope and the images collected using 1.6 NIH image. Results similar to those obtained with the anti-Cx43 mouse antibody from Alpha Diagnostics were obtained with an antibody made by Dr Birgit Rose to a peptide encompassing residues 252–271 in the C terminus of rat Cx43.

Patch-clamp recording

Patch electrodes were pulled from soda glass or borosilicate glass on a Brown Flaming programmable micropipette puller, and coated with wax to reduce electrode capacitance. Electrode resistance was 2–5 MΩ in normal physiological saline. Standard patch-clamp recording methods were used to measure whole-cell currents (Hamill *et al.*, 1981). Electrophysiological data were recorded with Axopatch amplifiers (models 1D, 200A; Axon Instruments) interfaced to a laboratory computer (Indec Systems) running programs written in BASIC-23 in this laboratory.

Saline compositions

Amphibian Physiological Saline (mM): 130 NaCl, 2.5 KCl, 3 $CaCl_2$, 1 $MgCl_2$, 10 Na-HEPES, 5 glucose, 5 Na pyruvate; pH 7.4, 278 mOsm. Intracellular saline (mM): 90 K-gluconate, 25 KCl, 3 $MgCl_2$, 10 Na-HEPES, 1 K_4BAPTA, 0.50 $CaCl_2$ (0.1 μM free Ca^{2+}), 2 mg/ml Lucifer yellow CH (dipotassium salt); pH 7.2, 250–260 mOsm. In some experiments 5 mg/ml biocytin was added to the intracellular saline.

Results

Dye-transfer between *Necturus* OSNs was noticed while recording whole-cell membrane currents with Lucifer yellow-filled patch pipettes. Transfer was seen between OSNs in epithelial slices and in small clusters of cells, suggesting the presence of inter-neuronal gap junction channels. This led us to question the role of gap junction channels in the olfactory epithelium and to examine their incidence.

Immunochemistry

Although connexins are well conserved through evolution (Bennett *et al.*, 1991, 1994), little is known about *Necturus* connexins. Antibodies to rat and mouse Cx43 cross-react well in human, chick and *Xenopus* tissues (Kumar and Gilula, 1996; Ball and McReynolds, 1998). A monoclonal antibody to rat Cx43 bound specifically to an epitope in the *Necturus* olfactory epithelium having the molecular weight of Cx43 (Figure 1). Immunolabeling was observed in the sensory regions of the nasal epithelium that included clusters of OSNs, supporting cells, and basal cells. The most intense label was in the basal half of the olfactory epithelium where the cell bodies of OSNs and basal cells are located. Label was located primarily on the plasma membranes and largely absent from the cytoplasm. Regions of non-sensory epithelium bordering the sensory clusters also showed labeling in cells adjacent to the basal lamina, but there was little label in the more apical region of the epithelium where support cell somata and OSN dendrites are found (Figure 1A). Control tissue treated with the secondary antibody alone showed comparatively little labeling suggesting a low level of nonspecific staining (Figure 1B). Western blots of the nasal sac showed a band at 43 kDa, which is where the band for Cx43 is expected. Incubation of the primary antibody with the control peptide eliminated this band. These results suggest that Cx43 is expressed in *Necturus* olfactory tissue, although it was not possible to determine the level of expression in olfactory neurons from tissue sections.

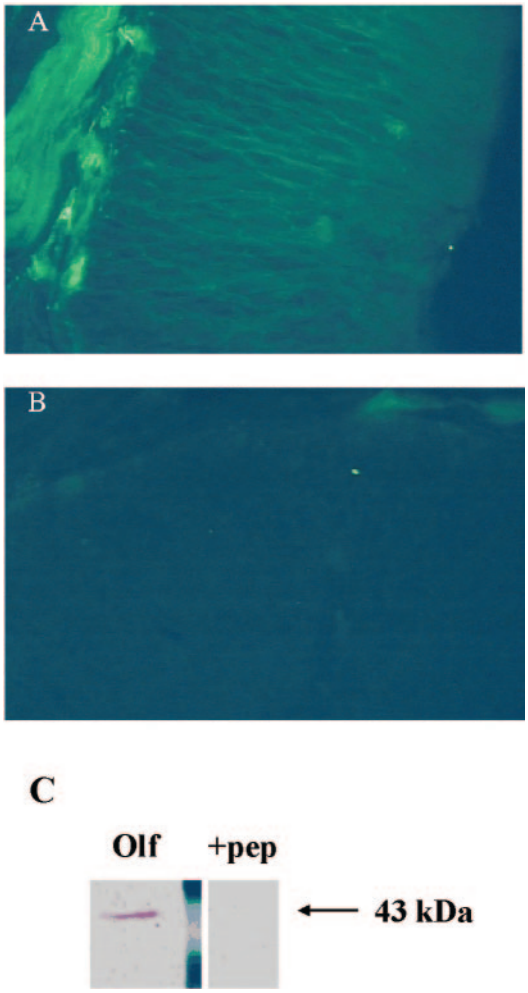

Figure 1 Connexin 43 labeling of olfactory tissue. (A) Section stained with an antibody for Cx43 and a FITC fluorescent secondary antibody. Staining extends from the apical surface of the epithelium (right) to the basal edge of the epithelium (left). Membranes of cells in the mid and lower portions of the epithelium were labeled; these are regions where the somata of OSNs and basal cells reside. Diffuse label in the apical half of the epithelium was seen where the dendrites of OSNs and the cell bodies of sustentacular cells are found. (B) A control section treated with the secondary antibody alone, fluorescent illumination. Only a trace amount of fluorescent labeling was observed. (C) Western blot of nasal sac tissue showed a band at approximately 43 kDa, the expected range for Cx43. Pretreatment of the primary antibody with the control peptide eliminated the band.

Capacitance measurements

Whole-cell capacitance was measured to estimate membrane surface area (nominally 1 μF/cm^2). The average capacitance of OSNs in slices was significantly greater than that of dissociated OSNs: 26.9 ± 4.98 pF (n = 100) (mean ± SD) compared with 16.3 ± 0.35 pF (n = 89), respectively, $P << 0.001$. Two plausible explanations for this difference are retained axonal membrane and intercellular coupling. Dissociated OSNs, unlike those in slice preparations, retain little or no axon. With a nominal axonal diameter near 1 μm, a 500 μm length of axon could account for the difference in capacitance if, during the measurement, its membrane potential were well-clamped. However, since the estimated length constant of the axon is 250–300 μm, it is likely that distal axon was not well clamped. As expected under these conditions, escape potentials were routinely observed in recordings from OSNs in slices but not from dissociated OSNs. This indicates that retained axonal membrane may only partially account for the capacitance difference. Intercellular coupling would offer an additional source of capacitance in slices. We also noted that the capacitance measurements from slices had a larger standard deviation than those from dissociated cells, a difference that could reflect variations in the length of retained axon, coupling between cells of variable size, or variations in intercellular coupling efficiency.

Dye-coupling

Intercellular coupling of OSNs was detected with Lucifer yellow CH (FW 443, Figure 2), an anionic dye that diffuses through most types of gap junction channels (Rao *et al.*, 1986; Hampson *et al.*, 1992). Dye-coupled OSNs were observed in slice preparations and small clusters of cells, but the incidence was low, and coupling of more than two cells was never seen. In a series of whole-cell recordings from OSNs in slices, coupling was detected in 3 of 32 cells (9%). To address concerns that Lucifer yellow may not permeate

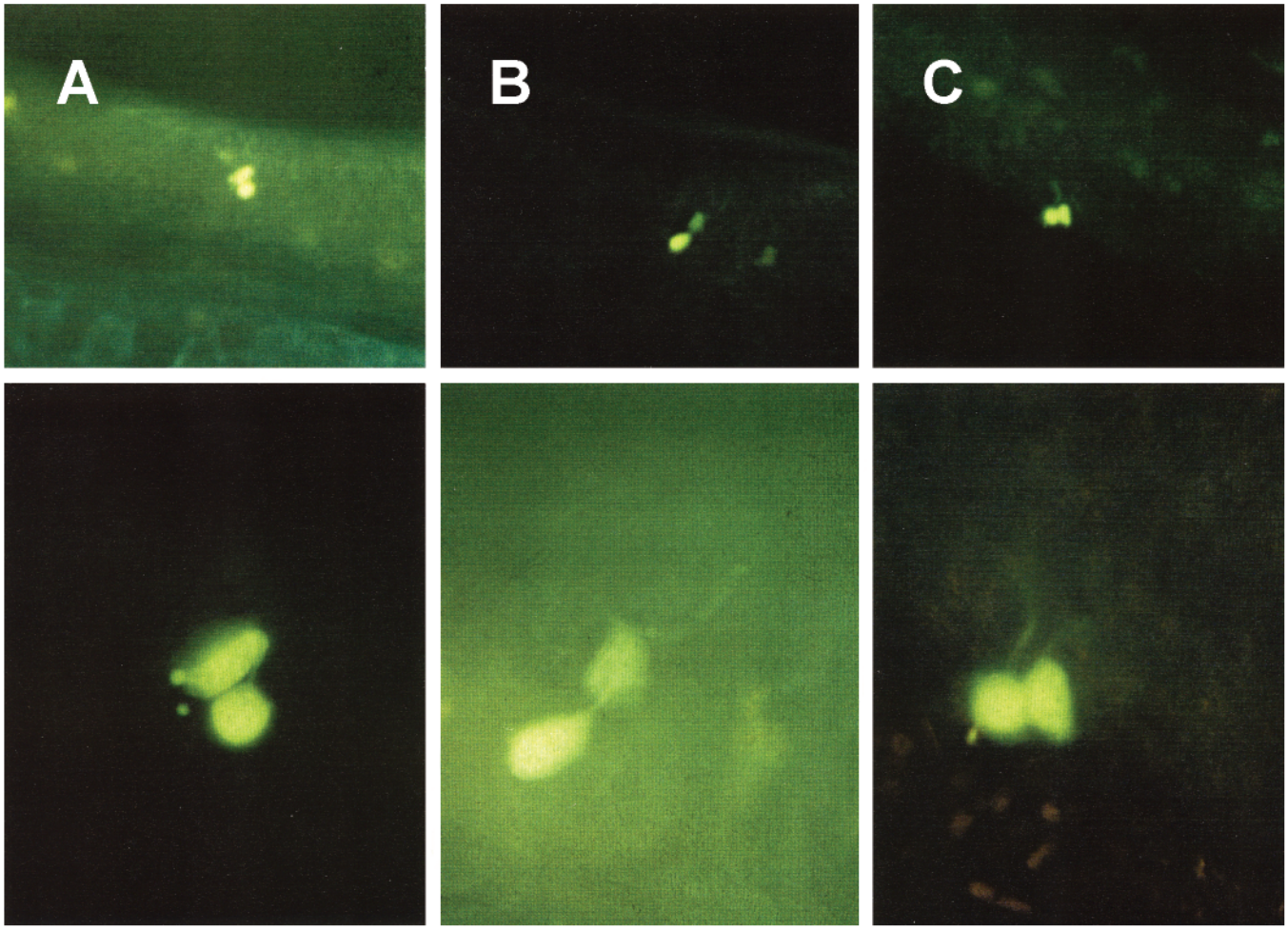

Figure 2 Three examples of dye-coupled cell pairs in the *Necturus* olfactory epithelium. Each pair was filled with Lucifer yellow dye during patch recording in a tissue slice, then photographed at 100× (upper panels) and 400× (lower panels) magnification after the electrode was removed. Whole-cell currents recorded while the cells were filling confirmed that the recorded cell of each pair was an OSN. The filled cell bodies, dendrites and axons could be seen by scanning up and down through the preparation.

all types of gap junction channels, we included Neurobiotin [*N*-(2-aminoethyl) biotinamide hydrochloride; Vector Laboratories, Burlingame, CA] with Lucifer yellow in 29 of the recordings. Neurobiotin, which is smaller (FW 322.8), is believed to permeate all gap junction channels (Kita and Armstrong, 1991). Evidence of additional coupling was not seen with Neurobiotin. Recorded cells were identified as OSNs from their morphology and voltage-gated currents; dye-coupling to non-neuronal cells was not observed.

Quantitative detection of coupling

Our dye-transfer results suggest that coupling between OSNs may be infrequent, although the capacitive and immunolabeling measurements may be interpreted otherwise. To examine the issue further, we designed experiments to measure changes in the apparent membrane capacitance and input resistance of presumptive cell pairs caused by blocking the coupling conductance. The input resistance and membrane capacitance of a cell can be estimated from the current that flows following a step change in membrane potential. If the cell is coupled to another cell by a gap junction, then the resistance and capacitance that will be measured reflect the values of both cells and depend on the magnitude of the coupling conductance. The effect of coupling is readily shown with a simple model.

We modeled a pair of cells coupled by a conductance G (Figure 3A). Assuming the cells were identical, we set $R' = R$ and $C' = C$. Measurements of either model cell in the absence of coupling would yield an input resistance R and membrane capacitance C; however, measurement of the coupled pair would yield 'apparent values' of resistance and capacitance that depend on G as follows:

$$R_{\text{app}} = \frac{R[RG+1]}{[2RG+1]}$$

$$C_{\text{app}} = \frac{C[2R^2G^2+2RG+1]}{[R^2G^2+2RG+1]}$$

These apparent values are plotted as a function of G in Figure 3A to the right of the model. As expected, with no

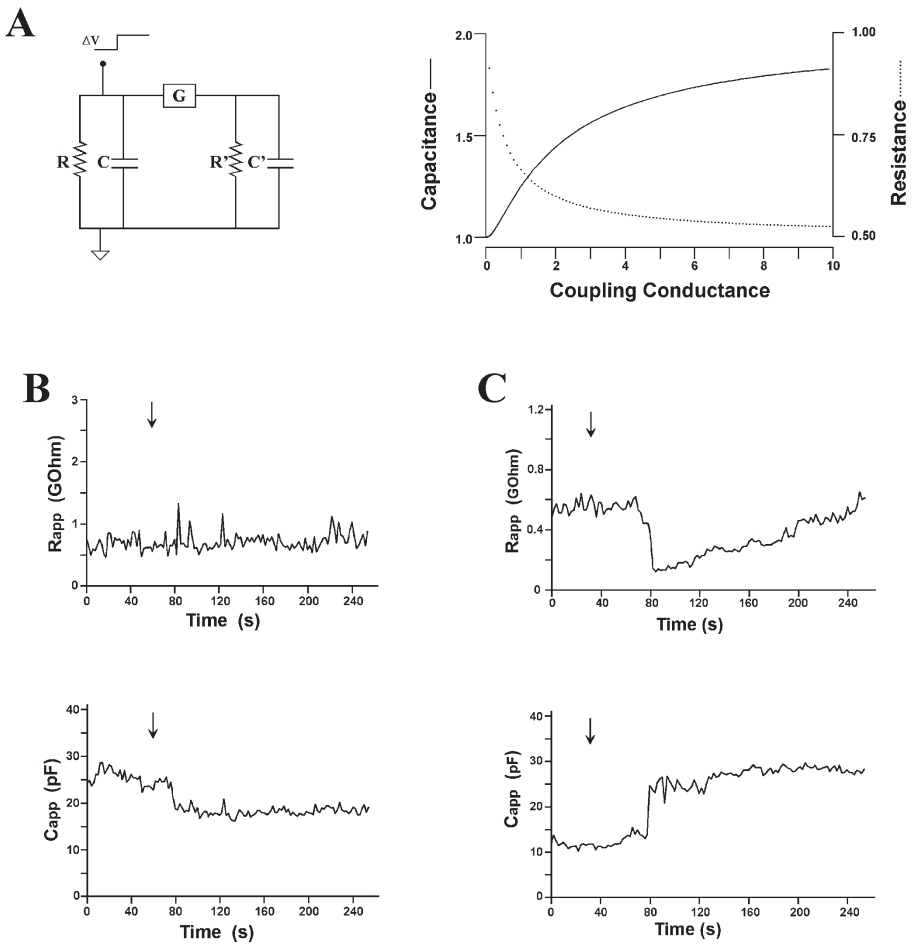

Figure 3 Modulating the intercellular coupling. **(A)** Modeling. A two-cell analog model was used to predict the dependence of apparent membrane resistance and capacitance on coupling conductance. The two cells, each modeled with a resistor in parallel with a capacitor (cell 1: *RC* and cell 2: *R′C′*), were coupled by a conductance element labeled *G*. The bottom of the analog corresponds to the outside of the cells which would be isopotential (bath potential). The top of the analog corresponds to the cytoplasmic side of the cells. A voltage step (shown being applied to the left-most cell) illustrates how the input resistance and membrane capacitance of a cell (or in this case two coupled cells) would be measured. In computing the apparent input resistance and membrane capacitance, we set $R = R'$ and $C = C'$. The dependencies of R_{app} and C_{app} on the coupling conductance are shown to the right of the model. The axes are plotted in multiples of *R* and *C*, respectively. The coupling conductance is plotted in multiples of $1/R$. **(B)** Apparent reduction of coupling by heptanol. Resistance (top) and capacitance (bottom) values were measured at 2 s intervals. Heptanol (1 mM) was introduced to the bath at the arrow. The measured capacitance abruptly decreased to a value similar to that of single OSNs. There was no apparent change in the input resistance. Here and in panel C, voltage pulses (17.5 ms long, 25 mV hyperpolarizing) were applied to an OSN in whole-cell mode to elicit current transients while holding the membrane potential at −70 mV. The transients, recorded at 2 s intervals, were used to estimate C_{app} and R_{app}. (C) Apparent increase in coupling caused by Ca^{2+} reduction. Calcium-free bath saline was introduced at the arrow. Shortly thereafter, C_{app} rose ~2-fold and R_{app} decreased, consistent with increased coupling.

coupling ($G = 0$), the apparent values reduce to the single cell values. However, as the coupling conductance increases, the values of C_{app} and R_{app} approach the limits $2C$ and $0.5R$, respectively. Notice that while both R_{app} and C_{app} depend nonlinearly on the coupling conductance, their dependencies are not identical. Most of the change in R_{app} occurs over the range $0 < G < 1/R$, while most of the change in C_{app} occurs as G increases beyond $1/R$. This suggests that agents which block gap junction channels should reveal the presence of coupling, since fully blocking the coupling conductance between two well-coupled cells should produce measurable changes in both C_{app} and R_{app}, while a partial block might strongly affect C_{app} but have much less effect on R_{app}.

Block by heptanol

The parameters C_{app} and R_{app} were measured from OSNs in slices during bath application of heptanol (1 mm) or octanol (0.55 mM), two long-chain aliphatic alcohols that block gap junction channels (Bastide *et al.*, 1995). The parameters were computed at 2 s intervals during recording using current transients elicited by 25 mV hyperpolarizing pulses. In 19 cells with initial values of C_{app} typical of slices (24.0 ± 1.9 pF, mean ± SD), the alcohols caused a decrease in C_{app} in only two cells (Figure 3B); in neither case was a significant change in R_{app} observed. The decrease in C_{app} had a rapid onset and slow washout similar to the time course of gap junction block reported in other studies (Bastide *et al.*, 1995). We

verified that the recorded cells were exposed to alcohol by the marked attenuation of voltage-gated Na^+ currents induced in every test cell.

Block by calcium

Gap junction channels are blocked by intracellular Ca^{2+} (Rose and Loewenstein, 1976), a feature that could explain a low incidence of observed coupling if intracellular [Ca^{2+}] were elevated under the conditions of our experiments. Slices of olfactory epithelium were exposed to low extracellular [Ca^{2+}] to alter Ca^{2+} homeostasis and lower the intracellular concentration. Coupling conductance was measured by recording C_{app} and R_{app} as above. If gap junction channels were blocked by Ca^{2+}, reducing [Ca^{2+}] should increase C_{app} and decrease R_{app}. Seven OSNs were tested with calcium-free APS; only 1 cell showed a simultaneous increase in C_{app} and decrease in R_{app} (Figure 3C) consistent with the unblock of closed gap junction channels.

Tracer loading through hemi-junctions

To further assess the incidence of coupling, we tested for tracer-permeable hemi-junctions in dissociated cells. This approach was used by DeVries and Schwartz (1992) to estimate the incidence of gap junctions in retinal horizontal cells. Dissociated cells from the olfactory epithelium were exposed to two tracers, Lucifer yellow CH or Neurobiotin, in the presence of low [Ca^{2+}] to open hemi-junctions. A tracer that permeated only gap junction channels should load the cells and be trapped when the cells were returned to normal Ca^{2+}. Loaded cells could then be counted. Controls were performed in parallel with each cell preparation, exposing cells to the tracer in the presence of normal Ca^{2+}. Working with dissociated cells permitted identification of OSNs by their distinct morphology and allowed ready detection of dye-loaded cells due to the low background of dye.

The results of 11 loading experiments are summarized in Table 1. The fraction of OSNs with gap junction channels opened by this procedure was low, on the order of 2–4%. Of particular note is the substantially greater filling of non-neuronal cells by Neurobiotin compared with Lucifer yellow, a difference that was not seen in OSNs. Given the caveat that the structural integrity of hemi-junction channels might well be compromised by dissociation, these numbers are regarded as lower limits of the incidence of gap junction channels.

Tracer injection by iontophoresis

To examine the extent of networks formed by coupling between OSNs, tracer molecules were iontophoretically injected into OSNs. In the retina, the injection of Lucifer yellow and Neurobiotin into amacrine cells revealed an extensive network of neurons as the tracers spread through the coupling junctions (Hampson *et al.*, 1992). Using thin slices (~300 μm thickness) and excised pieces of olfactory epithelium, OSNs were impaled with sharp microelectrodes (~100 MΩ) containing Lucifer yellow and Neurobiotin. These tracers were iontophoretically injected by passing a 0.5 nA alternating current for 3–5 min. The identification of OSNs was confirmed by their morphology after filling with Lucifer yellow. In pieces of excised tissue none of 14 injected OSNs were coupled, while in thin slices of olfactory epithelium, 3 of 68 injected OSNs (4.4%) showed coupling to one adjacent neuron. There was no evidence of a coupled network of OSNs beyond this.

Discussion

Gap junction channels in OSNs were first detected by electron microscopy in rat olfactory epithelia by Menco (1988). Later Miragall *et al.* (1992) found several connexins expressed in the mouse olfactory epithelium, but concluded the expression was in non-neuronal cells. Dye transfer through gap junctions between OSNs was first observed in land phase tiger salamanders following Lucifer yellow injection *in vivo* (Schwartz Levey *et al.*, 1992). Although coupling was seen only in pairs of OSNs, coupling between OSNs and non-neuronal cells was also reported. More recently Zhang and co-workers identified three connexins expressed in mouse OSNs: Cx36 (Zhang and Restrepo, 2003), Cx43 (Zhang *et al.*, 2000) and Cx45 (Zhang and Restrepo, 2002).

Table 1 Loading through hemi-junctions

	OSNs, low Ca^{2+}	OSNs, control	Other, low Ca^{2+}	Other, control
LY:	13 of 613 total	1 of 239 total	144 of 2434 total	58 of 2227 total
	2.1% overall	0.4% overall	5.3 ± 2.1%	2.6 ± 1.6%
NB:	8 of 206 total	0 of 154 total	1589 of 2589 total	674 of 2308 total
	3.9% overall	0% overall	64.9 ± 15.7%	28.1 ± 9.8%

Seven loading experiments were performed with Lucifer yellow CH (LY) and 4 with Neurobiotin. Both OSNs and non-neuronal cells ('other') were counted in plated aliquots of cell suspension. Because so few OSNs were filled in any one experiment (range: 0–7 in low Ca^{2+}), the counts from the experiments were summed and no statistics beyond the means were computed. For the non-neuronal cells, the numbers were sufficient that both the summed counts and the mean and standard deviation of the counts within experiments are given. Since low [Ca^{2+}] was expected to increase coupling, a one-tailed t test was used to compare the results of loading non-neuronal cells. The differences between the columns labeled 'Other' were significant with P values of 0.038 (Lucifer yellow) and 0.014 (Neurobiotin).

We found that Cx43 also appears to be expressed in *Necturus* OSNs. Gap junction channels have also been reported in mitral cells and granule cells in the adult olfactory bulb, where they appear to couple small networks of 6–8 or more neurons (Du *et al.*, 2002). Bulbar gap junctions contribute to the maintenance of network oscillations (Friedman and Strowbridge, 2003), suggesting that gap junction channels in the bulb may have a role in circuit function. As such they may contribute to odor processing with a role comparable to that of gap junction channels in the retina.

Gap junctions often seem enigmatic in neurons that rely on synaptic communication; however, gap junction channels have been found with increasing frequency in neurons. Nevertheless, the essential roles of the junctions have been difficult to establish. Recent work has focused on two areas: development (Rozental *et al.*, 2000; Leung *et al.*, 2002; Hanson and Landmesser, 2003) and the maintenance of local circuits (Carlen *et al.*, 2000; Sutor, 2002; Veruki and Hartveit, 2002). As neurons differentiate and develop, they elaborate growth cones and extend dendritic and axonal processes; gap junctions have been implicated in synchronizing these actions (Leung *et al.*, 2002). Gap junctions have also been found to control and regulate certain circuits of mature neurons; one of the best examples is in the retina where gap junction channels determine whether photoreceptor responses from rods or from cones are communicated to retinal ganglion output neurons (Baldridge *et al.*, 1998). In effect, retinal gap junctions optimize the eye for day or night vision.

The recognition that connexins were widely expressed in the olfactory epithelium suggested to us that they might optimize olfactory sensitivity in ways analogous to their role in the retina. If inter-neuronal gap junctions coupled OSNs into an extensive network, the propensity of OSNs to fire spontaneously would be reduced because coupling would lower each cell's input resistance. In effect, coupling would suppress spontaneous firing, resulting in a lower 'noise signal' coming from OSNs. Although electrical coupling of OSNs would also suppress odor-elicited firing, the excitability of individual OSNs could be rescued if their gap junction channels were closed during transduction. Closure of gap junction channels in retinal neurons is controlled by protein kinases. Thus regulation of olfactory gap junction channels during odor transduction could sharpen the odor signal without affecting sensitivity.

As a hypothesis, this scheme depends on the presence of functional gap junction channels in mature OSNs, not just on the expression of connexin subunits. We estimated that ~95% of OSNs in the *Necturus* olfactory epithelium are mature using a lifetime model with nominal values for the mean time-to-maturity (1 week) and mean lifetime of OSNs (20 weeks). This issue was recently examined experimentally in mice using antibodies to label markers of mature and immature OSNs (Iwema and Schwob, 2003). Of those OSNs that expressed a specific olfactory receptor protein, 2.4 ± 1.1% expressed the immature but not the mature marker; in contrast, in the general population of OSNs, without regard to the expression of olfactory receptor proteins, 12.1 ± 0.5% of OSNs expressed the immature but not the mature marker. Although the source of this disparity is unclear, the data suggest that ~90–95% of OSNs in adult mice are mature, similar to our estimate for OSNs in *Necturus*.

Although our results confirm that gap junction channels make intercellular connections between OSNs, the density and incidence of coupling in the *Necturus* olfactory epithelium was considerably less than 90%. Functional coupling was detected in only ~3–10% of the OSN population, and appeared to involve primarily pairs of OSNs. Our results give no evidence of an extended network of neurons, and they do not support a general role for gap junction channels in mature OSNs. However, our results would be consistent with a role for gap junction channels in the development of OSNs, although it is unclear what the channels might do in this regard. In a strict sense, our results indicate only that a small fraction of OSNs are functionally coupled by gap junctions, but they say nothing of the character of the coupled cells. Conceivably the coupled cells may comprise a population other than immature OSNs, such as senescent OSNs, diseased OSNs, or OSNs with a particular chemosensitivity.

Gap junctions in the olfactory epithelium are also expressed in non-neuronal sustentacular and basal cells (Menco, 1988; Miragall *et al.*, 1992; Schwartz Levey *et al.*, 1992). The incidence of tracer uptake through hemijunctions in non-neuronal cells in this study was higher than it was in OSNs, and the disparity was 10-fold greater using Neurobiotin than with Lucifer yellow. This difference suggests that the gap junction channels expressed by non-neuronal cells are unlike those in OSNs. The likely explanation is different connexins. By comparison, Lucifer yellow and Neurobiotin showed similar uptake rates in OSNs, indicating that the low incidence of dye coupling with Lucifer yellow that we found between OSNs was not a consequence of Lucifer yellow being a relatively poor tracer.

Anti-Cx43 staining appeared more widespread than the incidence of coupled OSNs in the olfactory epithelium. Moreover, the staining was neither confined to neurons, nor punctate as might be expected of gap junctions. This suggests that not all the Cx43 immunolabel represented functional gap junction channels. An additional factor that we could not test may also have contributed to the difference between immunostaining and coupling: many gap junction channels may have been closed. The gating of gap junction channels in the retina and elsewhere is controlled in part by phosphorylation (Mills and Massey, 1995; Lampe and Lau, 2000), and Cx43 can be phosphorylated by both protein kinases A and C (Shah *et al.*, 2002). If the gating of olfactory gap junction channels were controlled by phosphorylation,

the channels may have been closed under the conditions of our recordings. In several experiments we pre-exposed slice preparations to either a phosphodiesterase inhibitor (isobutyl methylxanthine, 21 cells), a protein kinase A inhibitor (H-89, five cells), or an adenylyl cyclase inhibitor (MDL-12,330A, 13 cells, land phase tiger salamander), but saw no change in the incidence of coupling (data not shown), suggesting that closed gap junction channels were unlikely to explain the low incidence of inter-neuronal coupling in the olfactory epithelium.

Conclusion

Our experiments show that Cx43 is expressed in the nasal sacs of *Necturus maculosus*, where functional gap junction channels connect a small percentage of the OSNs. The low incidence of coupled neurons suggests that gap junction channels do not have a role in processing or controlling transmission of odor information in mature OSNs, but the channels may be important, for example, in the development of new sensory neurons or in functions specific to other subsets of OSNs.

Acknowledgements

This work was supported by grant DC03146 to VED from the National Institutes of Health.

References

Baldridge, W.H., Vaney, D.I. and **Weiler, R.** (1998) *The modulation of intercellular coupling in the retina.* Semin. Cell Dev. Biol., 9, 311–318.

Ball, A.K. and **McReynolds, J.S.** (1998) *Localization of gap junctions and tracer coupling in retinal Muller cells.* J. Comp. Neurol., 393, 48–57.

Bastide, B., Herve, J.C., Cronier, L. and **Deleze, J.** (1995) *Rapid onset and calcium independence of the gap junction uncoupling induced by heptanol in cultured heart cells.* Pflugers Arch., 429, 386–393.

Bennett, M.V., Barrio, L.C., Bargiello, T.A., Spray, D.C., Hertzberg, E. and **Saez, J.C.** (1991) *Gap junctions: new tools, new answers, new questions.* Neuron, 6, 305–320.

Bennett, M.V., Zheng, X. and **Sogin, M.L.** (1994) *The connexins and their family tree.* Soc. Gen. Physiol Ser., 49, 223–233.

Bigiani, A. and **Roper, S.D.** (1991) *Mediation of responses to calcium in taste cells by modulation of a potassium conductance.* Science, 252, 126–128.

Bigiani, A. and **Roper, S.D.** (1995) *Estimation of the junctional resistance between electrically coupled receptor cells in* Necturus *taste cells*. J. Gen. Physiol., 106, 705–725.

Bruzzone, R., White, T.W. and **Paul, D.L.** (1996) *Connections with connexins: the molecular basis of direct intercellular signaling.* Eur. J. Biochem., 238 , 1–27.

Carlen, P.L., Skinner, F., Zhang, L., Naus, C., Kushnir, M. and **Perez Velazquez, J.L.** (2000) *The role of gap junctions in seizures.* Brain Res. Rev., 32, 235–241.

DeVries, S.H. and **Schwartz, E.A.** (1992) *Hemi-gap-junction channels in solitary horizontal cells of the catfish retina.* J. Physiol., 445, 201–230.

Du, J., Maloney, R.E. and **Hamilton, K.A.** (2002) *Video-microscopic analysis of dye coupling in the salamander olfactory bulb.* J. Neurosci. Res., 68, 385–397.

Dubin, A.E. and **Dionne, V.E.** (1993) *Modulation of Cl–, K+ and non-selective cation conductances by taurine in olfactory receptor neurons of the mudpuppy* Necturus maculosus. J. Gen. Physiol., 101, 469–485.

Friedman, D. and **Strowbridge, B.W.** (2003) *Both electrical and chemical synapses mediate fast network oscillations in the olfactory bulb.* J. Neurophysiol., 89, 2601–2610.

Goodenough, D.A., Goliger, J.A. and **Paul, D.L.** (1996) *Connexins, connexons, and intercellular communication.* Annu. Rev. Biochem., 65, 475–502.

Graziadei, P.P. and **Monti Graziadei, G.A.** (1976) *Olfactory epithelium of* Necturus maculosus *and* Ambystoma tigrinum. J. Neurocytol., 5, 11–32.

Hamill, O.P., Marty, A. Neher, E., Sakmann, B. and **Sigworth, F.S.** (1981) *Improved patch-clamp techniques for high resolution current recording from cells and cell-free membrane patches.* Pflugers Arch., 391, 85–100.

Hampson, E.C., Vaney, D.I. and **Weiler, R.** (1992) *Dopaminergic modulation of gap junction permeability between amacrine cells in mammalian retina.* J. Neurosci., 12, 4911–4922.

Hanson, M.G. and **Landmesser, L.T.** (2003) *Characterization of the circuits that generate spontaneous episodes of activity in the early embryonic mouse spinal cord.* J. Neurosci., 23, 587–600.

Iwema, C.L. and **Schwob, J.E.** (2003) *Odorant receptor expression as a function of neuronal maturity in the adult rodent olfactory system.* J. Comp Neurol., 459, 209–222.

Kita, H. and **Armstrong, W.** (1991) *A biotin-containing compound* N-*(2-aminoethyl)biotinamide for intracellular labeling and neuronal tracing studies: comparison with biocytin.* J. Neurosci. Methods, 37, 141–150.

Kumar, N.M. and **Gilula, N.B.** (1996) *The gap junction communication channel.* Cell, 84, 381–388.

Lampe, P.D. and **Lau, A.F.** (2000) *Regulation of gap junctions by phosphorylation of connexins.* Arch. Biochem. Biophys., 384, 205–215.

Leung, D.S., Unsicker, K. and **Reuss, B.** (2002) *Expression and developmental regulation of gap junction connexins Cx26, Cx32, Cx43 and Cx45 in the rat midbrain-floor.* Int. J. Dev. Neurosci., 20, 63–75.

Menco, B.P. (1988) *Tight-junctional strands first appear in regions where three cells meet in differentiating olfactory epithelium: a freeze-fracture study.* J. Cell Sci., 89, 495–505.

Mills, S.L. and **Massey, S.C.** (1995) *Differential properties of two gap junctional pathways made by AII amacrine cells.* Nature, 377, 734–737.

Miragall, F., Hwang, T.-K., Traub, O., Hertzberg, E.L. and **Dermietzel, R.** (1992) *Expression of connexins in the developing olfactory system of the mouse.* J. Comp. Neurol., 325, 359–378.

Rao, G., Barnes, C.A. and **McNaughton, B.L.** (1986) *Intracellular fluorescent staining with carboxyfluorescein: a rapid and reliable method for quantifying dye-coupling in mammalian central nervous system.* J. Neurosci. Methods, 16, 251–263.

Rose, B. and **Loewenstein, W.R.** (1976) *Permeability of a cell junction and the local cytoplasmic free ionized calcium concentration: a study with aequorin.* J. Membr. Biol., 28, 87–119.

Rozental, R., Srinivas, M., Gokhan, S., Urban, M., Dermietzel, R., Kessler, J.A., Spray, D.C. and **Mehler, M.F.** (2000) *Temporal expression of neuronal connexins during hippocampal ontogeny.* Brain Res. Rev., 32, 57–71.

Schwartz Levey, M., Cinelli, A.R. and **Kauer, J.S.** (1992) *Intracellular injection of vital dyes into single cells in the salamander olfactory epithelium.* Neurosci. Lett., 140, 265–269.

Shah, M.M., Martinez, A.M. and **Fletcher, W.H.** (2002) *The connexin43 gap junction protein is phosphorylated by protein kinase A and protein kinase C:* in vivo *and* in vitro *studies.* Mol. Cell Biochem., 238, 57–68.

Sutor, B. (2002) *Gap junctions and their implications for neurogenesis and maturation of synaptic circuitry in the developing neocortex.* Results Probl. Cell Differ., 39, 53–73.

Veruki, M.L. and **Hartveit, E.** (2002) *AII (Rod) amacrine cells form a network of electrically coupled interneurons in the mammalian retina.* Neuron, 33, 935–946.

Weiler, E. and **Farbman, A.I.** (1997) *Proliferation in the rat olfactory epithelium: age-dependent changes.* J. Neurosci., 17, 3610–3622.

Zhang, C., Finger, T.E. and **Restrepo, D.** (2000) *Mature olfactory receptor neurons express connexin 43.* J. Comp Neurol., 426, 1–12.

Zhang, C. and **Restrepo, D.** (2002) *Expression of connexin 45 in the olfactory system.* Brain Res., 929, 37–47.

Zhang, C. and **Restrepo, D.** (2003) *Heterogeneous expression of connexin 36 in the olfactory epithelium and glomerular layer of the olfactory bulb.* J. Comp Neurol., 459, 426–439.

Accepted October 26, 2003